Title

Metabolic Reprogramming Regulates the Proliferative and Inflammatory Phenotype of Adventitial Fibroblasts in Pulmonary Hypertension Through the Transcriptional Corepressor C-Terminal Binding Protein-1

Journal

Circulation, 134(15)

ISSN

0009-7322

Authors

Li, Min
Riddle, Suzette
Zhang, Hui
et al.

Publication Date

2016-10-11

DOI

10.1161/circulationaha.116.023171

Peer reviewed

Published in final edited form as:

Circulation. 2016 October 11; 134(15): 1105–1121. doi:10.1161/CIRCULATIONAHA.116.023171.

Metabolic Reprogramming Regulates the Proliferative and Inflammatory Phenotype of Adventitial Fibroblasts in Pulmonary Hypertension Through the Transcriptional Co-Repressor C-terminal Binding Protein-1

Min Li, PhD[1], **Suzette Riddle, PhD**[1], **Hui Zhang, MD, PhD**[1], **Angelo D'Alessandro, PhD**[2], **Amanda Flockton, BS**[1], **Natalie J. Serkova, MD**[3], **Kirk C. Hansen, PhD**[2], **Radu Moldvan, PhD**[4], **B. Alexandre McKeon, MS**[1], **Maria Frid, PhD**[1], **Sushil Kumar, PhD**[1], **Hong Li, PhD**[5], **Hongbing Liu, MD, PhD**[5], **Angela Cánovas, PhD**[9], **Juan F. Medrano, PhD**[10], **Milton G. Thomas, PhD**[11], **Dijana Iloska, MSc**[8], **Lydie Plecita-Hlavata, PhD**[7], **Petr Ježek, PhD**[7], **Soni Pullamsetti, PhD**[8], **Mehdi A. Fini, PhD**[1], **Karim C. El Kasmi, MD, PhD**[6], **Qinghong Zhang, PhD**[5], and **Kurt R. Stenmark, MD**[1]

[1]Pediatric Critical Care Medicine/CVP Research, University Colorado Denver, CO

[2]Department of Biochemistry and Molecular Genetics and Biological Mass Spectrometry Shared Resource, University Colorado Denver, CO

[3]Department of Anesthesiology, University Colorado Denver, CO

[4]Advanced Light Microscopy Core Facility, University Colorado Denver, CO

[5]Department of Dermatology, University Colorado Denver, CO

[6]Department of Pediatrics, Division of Gastroenterology, Hepatology, and Nutrition, University Colorado Denver, CO

[7]Department of Mitochondrial Physiology, Institute of Physiology, Czech Academy of Sciences, Prague, Czech Republic

[8]Department of Lung Development and Remodeling, Max-Planck-Institute for Heart and Lung Research, Bad Nauheim, Germany

[9]Center for Genetic Improvement of Livestock, Department of Animal Bioscience, University of Guelph, Guelph, Ontario, Canada

[10]Department of Animal Science, University of California-Davis, Davis, CA

[11]Department of Animal Science, Colorado State University, Fort Collins, CO

Abstract

Background—Changes in metabolism have been suggested to contribute to the aberrant phenotype of vascular wall cells including fibroblasts in pulmonary hypertension (PH). Herein, we

Address for Correspondence: Kurt R. Stenmark, MD, Pediatric Critical Care Medicine/CVP Research, University of Colorado Denver, 12700 E 19th Ave., RC2, B131, Aurora, CO 80045, Tel: 303-724-5620, Fax: 303-724-5628, Kurt.Stenmark@ucdenver.edu.

Conflict of Interest Disclosures: The authors have no conflict of interests.

test the hypothesis that metabolic reprogramming to aerobic glycolysis is a critical adaptation of fibroblasts in the hypertensive vessel wall that drives proliferative and pro-inflammatory activation through a mechanism involving increased activity of the NADH-sensitive transcriptional co-repressor C-terminal binding protein 1 (CtBP1).

Methods—RNA-Sequencing, qPCR, ^{13}C-NMR, fluorescence-lifetime imaging, mass spectrometry-based metabolomics and tracing experiments with U-^{13}C-glucose were used to assess glycolytic reprogramming and to measure NADH/NAD$^+$ ratio in bovine and human adventitial fibroblasts, and mouse lung tissues. Immunohistochemistry was utilized to assess CtBP1 expression in the whole lung tissues. CtBP1 siRNA and the pharmacologic inhibitor 4-methylthio-2-oxobutyric acid (MTOB) were utilized to abrogate CtBP1 activity in cells and hypoxic mice.

Results—We found adventitial fibroblasts from calves with severe hypoxia-induced PH and humans with IPAH (PH-Fibs) displayed aerobic glycolysis when cultured under normoxia, accompanied by increased free NADH and NADH/NAD$^+$ ratios. Expression of the NADH sensor CtBP1 was increased *in vivo* and *in vitro* in fibroblasts within the pulmonary adventitia of humans with IPAH and animals with PH and cultured PH-Fibs, respectively. Decreasing NADH pharmacologically with MTOB, or genetically blocking CtBP1 using siRNA, upregulated the cyclin-dependent genes (p15 and p21) and pro-apoptotic regulators (NOXA and PERP), attenuated proliferation, corrected the glycolytic reprogramming phenotype of PH-Fibs, and augmented transcription of the anti-inflammatory gene *HMOX1*. ChIP analysis demonstrated that CtBP1 directly binds the *HMOX1* promoter. Treatment of hypoxic mice with MTOB decreased glycolysis and expression of inflammatory genes, attenuated proliferation, and suppressed macrophage numbers and remodeling in the distal pulmonary vasculature.

Conclusions—CtBP1 is a critical factor linking changes in cell metabolism to cell phenotype in hypoxic and other forms of PH and a therapeutic target.

Keywords

proliferation; glycolysis; inflammation; heme oxygenase; apoptosis

Journal Subject Terms

Pulmonary Hypertension

Pulmonary hypertension (PH) is a devastating syndrome with high mortality, affecting both pediatric and adult patients with a wide variety of disorders [1]. The pulmonary vasculature in these patients exhibits significant cellular and structural changes within the intima, media, and adventitia that include augmented proliferation, resistance to apoptosis, and increased production of inflammatory mediators and extracellular matrix proteins [2]. These cellular changes are recapitulated, at least in part, in various animal models of PH [3]. Notably, some of the earliest pathophysiological changes are observed in the pulmonary artery adventitia and include robust proliferation of fibroblasts and accumulation of macrophages [4–7]. These phenotypic changes in adventitial fibroblasts are maintained *ex vivo* over multiple passages in culture and are, in part, regulated through epigenetic mechanisms [4, 5, 7–9]. Collectively,

these observations are consistent with the hypothesis that many of the cellular and molecular features of PH resemble hallmark characteristics of cancer [10, 11].

It is increasingly recognized that increased proliferation and inflammatory activation can occur in the context of changes in cellular metabolism toward aerobic glycolysis (the "Warburg effect") and that there is an intimate link between metabolic adaptation and functional cellular phenotype[12, 13]. Importantly, metabolic changes closely resembling those of cancer cells have been reported in PH in endothelial cells, smooth muscle cells, and most recently fibroblasts, and have formed the basis for a "metabolic theory of PH" [12, 14]. Further, findings using *in vivo* non-invasive imaging approaches support the hypothesis that the ^{18}FDG PET signal originated in the adventitia where activated fibroblasts and macrophages are observed [14]. However, the mechanisms that link metabolic reprograming to inflammatory and proliferative pathways in PH remain largely unknown.

C-terminal binding protein (CtBP) comprises a dimeric family of transcriptional repressors encoded by two paralogous genes (*CTBP1* and *CTBP2*) that have major roles in animal cell development and cancer and have been suggested to be "sensors" of the metabolic state of cells that can modulate many aspects of cell phenotype [15]. Overexpression of CtBP is observed in a number of cancers, including prostate, ovarian, colon, and breast [16–18]. Studies in cancer and nervous system revealed that CtBPs promote cellular survival primarily through repression of Bcl-2 family members and other pro-apoptotic molecules (PERP, Bax, Bik, Puma, p21, and Noxa), as well as tumor suppressors (e.g. p16INK4a, p15 INK4b) [15, 18, 19]. Importantly, there is emerging evidence that CtBPs may also function to modulate the inflammatory response [20]. Further, a recent genome-wide analysis in breast cancer provided a more comprehensive description of CtBP repression targets [18, 21].

CtBP targets were categorized into three main categories: genes that regulate cell renewal and pluripotency, genes that control genome stability, and genes that regulate epithelial differentiation and prevent epithelial-to-mesenchymal transition (EMT), all processes of potential importance in PH pathogenesis [18, 21]. CtBP is unique among transcription factors in the incorporation of a D-isomer specific 2-hydroxyacid dehydrogenase (D2-HDH) domain, which reduces or oxidizes substrates utilizing the coenzyme NADH[15, 18]. CtBP recruitment of coenzyme NAD+ or NADH induces dimerization, an event necessary for transcriptional repressor activity, linking enzymatic function and transcriptional activity. Although both forms of this dinucleotide are capable of inducing CtBP dimerization, CtBPs bind NADH with up to 100-fold higher affinity than NAD^+, suggesting that these proteins are in fact sensitive to the ratio of NADH to NAD^+ within the nucleus [22, 23]. Thus, metabolic changes in cells that favor increases in free NADH (such as hypoxia or aerobic glycolysis) activate CtBPs and lead to transcriptional repressor activity. CtBPs may thus be an example of how cellular metabolic status can influence epigenetic control of cell function and fate.

Here, we sought to test a novel hypothesis that in PH the metabolic/redox sensor CtBP1 drives persistent pro-proliferative, anti-apoptotic and pro-inflammatory activation of pulmonary adventitial fibroblasts by linking metabolic reprogramming (aerobic glycolysis and subsequently increased NADH) to gene transcription. Our approach was first to use RNA-Seq to determine whether metabolic pathways differ between control (CO-Fibs) and

pulmonary hypertensive (PH-Fibs). We then performed a detailed metabolic evaluation of both CO- and PH-Fibs cultured under normoxic conditions using NMR and MS (steady state and tracing experiments with ^{13}C-glucose). We assessed NADH directly using mass spectrometry and also with Fluorescence Lifetime Imaging (FLIM) in cultured fibroblasts. CtBP1 expression was also evaluated by qPCR and immuno-staining approaches. We assessed CtBP1's functional role in controlling cell phenotype utilizing both genetic (siRNA) and a novel pharmacologic inhibitor of CtBP1: 4-methylthio-2-oxobutyric acid (MTOB), a substrate of CtBP dehydrogenase, which has recently been shown to antagonize CtBP transcriptional regulation [18, 24]. Finally, using a hypoxic mouse model of PH, we treated mice with MTOB to prove the concept that CtBP1 could serve as a therapeutic target to inhibit hypoxia-induced cell proliferation and inflammation.

Methods

A detailed Methods section is provided in the Supplement Materials.

Animals

Neonatal calves and C57BL/6 mice exposed to chronic hypoxia were used in this study. All animal procedures were performed in accordance with the Guidelines for Animal Experimentation established and approved by the University of Colorado Anschutz Medical Campus and Colorado State University IRBs.

Tissue Specimen

Lung tissues from hypertensive and control calves (n= 5–7, each group) and mice (n= 5, each group) were used for RT-PCR, immunohistochemical/immunofluorescent staining analyzes. Human lung tissue specimens from subjects with idiopathic pulmonary arterial hypertension (IPAH) (n =7) or donor controls (n = 8) were obtained during lung transplantation and used for qPCR and immunohistochemical staining analysis. The study protocol for tissue donation was approved by the ethics committee (Ethik Kommission am Fachbereich Humanmedizin der Justus Liebig Universität Giessen) of the University Hospital Giessen (Giessen, Germany) in accordance with national law and with Good Clinical Practice/International Conference on Harmonization guidelines. Written informed consent was obtained from each individual patient or the patient's next of kin (AZ 31/93).

Cell Culture

Isolation of adventitial fibroblasts from distal pulmonary arteries of hypertensive and control calves was performed as described in Methods on-line. Human pulmonary artery fibroblasts were derived from patients with IPAH or from control donors undergoing lobectomy or pneumonectomy. All cells were cultured under normoxic conditions. Experiments were performed on cells at passages 5–10.

RNA Sequencing (RNA-Seq)

RNA from bovine CO-Fibs and PH-Fibs (n=6, each group) were used to perform RNA-Sequencing analysis. Total RNA was purified, fragmented, and converted to cDNA. Sequencing libraries were made with the TruSeq RNA Sample Preparation kit (Illumina, San

Diego, CA). RNA-Sequencing was performed on a HiSeq2000 sequencer analyzer. Sequence reads were assembled to the annotated UMD3.1 bovine reference genome (http://www.ncbi.nlm.nih.gov/genome/?term=bos+taurus). Quality control analysis was performed using the CLC Genomics workbench software (CLC Bio, Aarhus, Denmark). All the samples analyzed passed all the QC parameters, indicating a very good quality.

Data was normalized by calculating the 'reads per kilo base per million mapped reads' (RPKM) for each gene. The statistical analysis was performed using the total exon reads as expression values by the empirical analysis of differential gene expression (EDGE) tool of CLC Bio Genomic workbench software. This tool is based on the EdgeR Bioconductor package and uses count data (i.e. total exon reads) for the statistical analysis. Genes were filtered based on minimum expression greater than 0.2 RPKM. False discovery rate (FDR) was used for multiple testing corrections. Finally, differentially expressed genes were selected based on fold-change (equal or higher to 2), P-value ($p<0.01$), and FDR value ($q<0.1$). A detailed method is provided in the Supplemental Materials.

Real-Time RT-PCR

Total RNA from cultured cells was isolated using Qiagen Mini Kit (Qiagen, Valencia, CA). Total RNA from tissues was isolated with Trizol. The sequences for all primers are listed in Suppl. Table 1. Results are presented as fold change using delta-delta Ct method.

Quantitative Multinuclear Magnetic Resonance (NMR) Metabolomics and ^{13}C-glucose Fluxes

Fibroblasts were incubated with 10 mM of $^{13}C_1$-glucose (glucose with ^{13}C at C_1 position, Cambridge Isotope Laboratories, Tewksbury, MA) as the exclusive glucose source (and otherwise under standard growth conditions). After 24 hrs cells were perchloric acid extracted and used for NMR analysis. High-resolution ^{1}H-, ^{31}P- and ^{13}C-NMR experiments were performed using Bruker 400 MHz Avance III spectrometer (Bruker BioSpin, Fremont, CA). In cell extracts, intracellular ^{13}C-glucose and its ^{13}C-labeled products from glycolysis and the TCA cycle were calculated from ^{13}C-NMR spectra. Spectra acquisition and metabolite integration were performed using Bruker TopSpin software. Metabolite identification and multivariate partial least squares-discriminant analysis (PLS-DA) were performed using the Human metabolome database (HMDB). Data were normalized to cell mass.

UHPLC-Mass Spectrometry-Based direct NADH measurements and Metabolomics Analyses: steady state and U-^{13}C-glucose tracing experiments

CO- and PH-Fibs (n=3, each group), either cultured in normal media or media supplemented with 10 mM U-^{13}C-glucose (Cambridge Isotope Laboratories, Tewksbury, MA) for 5 min, 1, 8 and 24h were extracted (2×10^6 cells/ml buffer) and run through a C18 reversed phase column (Phenomenex, Torrance, CA) through an ultra-high performance chromatographic system (UHPLC - Vanquish, Themo Fisher). Metabolite assignment, peak integration for relative quantitation and isotopologue distributions in tracing experiments were calculated through the software Maven (Princeton), against the KEGG pathway database and an in-house validated standard library (>650 compounds – also including NADH – product no.

N8129 - SIGMA Aldrich; IROATech). To determine linearity (r^2 >0.99) and sensitivity of the approach (LOD and LOQ), NADH was weighed and progressively diluted (from 0.5 to 5000 injected pmol range – 4 orders of magnitude) before injection through UHPLC-MS. Integrated peak areas were exported into Excel (Microsoft, Redmond, CA) for statistical analysis (t-test, ANOVA through the software GraphPad Prism.

Frozen mouse whole lung tissues were snap-frozen, powered and weighed in the presence of liquid nitrogen and dry ice, and cold lysis buffer (10mg tissue/ml buffer) was added. Samples were extracted at 4°C for 30min, centrifuged, and the supernatants were used for metabolomics analysis as described above. Data was normalized by tissue mass.

Assessment of NADH/NAD$^+$ Ratio

NADH/NAD$^+$ ratio was determined with an enzymatic cycling reaction using modified methods by Williamson as described in Methods online.

Fluorescence Lifetime Imaging (FLIM)

To directly visualize NADH level in cells, FLIM of two-photon excited NADH was performed at the UCD Advanced Light Microscopy Core.

Inhibition of CtBP1

CtBP1 was inhibited either genetically by siRNA or pharmaceutically by 4-Methylthio 2-oxobutyric acid (MTOB). Transfection efficiencies were shown in Suppl. Fig. 1.

Cell Proliferation Assay

An equal number of cells were plated onto 24-well plates in full DMEM supplemented with 10% calf serum (CS) for bovine cells, or with 10% fetal calf serum (FCS), for human cells, and then treated with 2-deoxy-glucose (2-DG, 10 mM), pyruvate (20 mM), MTOB, 2.5 mM, CtBP1 siRNA (50 nM), scrambled siRNA, or left untreated. Cell numbers were counted, in triplicate wells, on days 1, 2, and 3. In parallel, cells with each type of treatment were collected for RT-PCR.

Chromatin Immunoprecipitation (ChIP) Assay

ChIP assay was used to study CtBP1 protein interaction with its target gene. Human fibroblasts were cross-linked with ice cold 1% formaldehyde for 15min, and the reaction was stopped by adding 0.125M glycine. Cell lysates were centrifuged, and the pellet was sonicated in lysis buffer to shear DNA. Fragmented DNA was precipitated with CtBP1 antibody (EMD Millipore, Billerica MA) using immobilized recombinant protein A affinity resins (RepliGen. Waltham, MA). Unbound DNA fragments were washed off, and beads were removed with elution buffer. Precipitated protein/DNA complexes were reverse cross-linked by adding 350mM NaCl and incubated for 6hrs at 65°C. DNA was then purified and used for PCR analysis.

Statistical Analysis

Prism software version 5 (GraphPad, Software, Inc., www.graphpad.com) was used for t-test or ANOVA followed by Bonferroni post-test analysis.

Values were expressed as mean ± SEM. For basic comparisons of two gaussian distributed sample sets, we used student t-tests. When comparing multiple groups, the respective ANOVA Analysis (one way when comparing one characteristic, or two way if two dependent variables where involved) was performed. P-values were subject to multiple testing adjustment using Bonferroni correction. Supervised partial least square-discriminant analysis (PLS-DA, Simca, Umetrics, San Jose, CA) were used to determine the variance of metabolic phenotypes in CO- and PH-Fibs, as determined via NMR and MS analyses and were sufficient to discriminate biological samples. To validate partial least square-discriminant analysis, random permutations were performed through MetaboAnalyst and Multibase (20 random permutations were selected (significance threshold 0.05, <100 variables tested). False discovery rate (Benjamini Hochberg) was <0.1 for all significant metabolites. Power analysis was performed to make sure that the number of replicates was sufficient to ensure >80% probability to have a FDR<0.1 for all the significant observations (tested through MetaboAnalyst 3.0). Differences with *P* values less than 0.05 were considered statistically significant.

Results

PH-Fibs are metabolically reprogrammed to aerobic glycolysis

RNA-Seq analysis elucidated over 1000 differentially regulated genes in bovine PH-Fibs in comparison to CO-Fibs (n=6, each group, $p<0.01$, fold change >2). Glycolysis/Gluconeogenesis and pyruvate metabolism were identified as two of the most significantly up-regulated pathways (Table 1, Suppl. Fig. 2A). In particular, 9 genes code for enzymes and transporters involved in glucose-to-lactate catabolism were up-regulated in PH-Fibs (Table 2).

Validation by RT-PCR analysis confirmed increased gene expression of the glycolytic genes *GLUT1*, *HK2*, and *LDHA* in both bovine and human PH-Fibs relative to CO-Fibs (Fig. 1A). In addition, up-regulation of *GLUT1*, *GLUT4*, *G6PD* genes (as well as HK2 and LDHA, which are submitted as part of another manuscript), was observed in vessels isolated by LCM of IPAH patients when compared to controls (Fig. 1B). Further, up-regulation of GLUT1 protein expression was observed *in situ* in the adventitia of hypoxic hypertensive calves by immunofluorescence (Fig. 1C), and *in vitro* in cultured bovine and human PH-Fibs by western blot (Fig. 1D).

Nuclear magnetic resonance (NMR) and mass spectrometry (MS)-based metabolomics analyses confirmed transcriptomics results, showing that significantly different metabolic phenotypes exist between CO-Fibs and PH-Fibs (Suppl. Fig. 2B–C, 3A–B), as well as metabolic reprogramming to aerobic glycolysis in PH-Fibs (Fig. 2, Suppl. Fig. 2, 3). Glycolytic changes included increased glucose uptake, generation of sugar phosphates, ^{13}C-glycolytic signature, ^{13}C-lactate (from $^{13}C_1$-glucose steady state NMR analyses –Suppl. Fig.

2C, Suppl. Fig. 3C–D); increased D-glucose, glyceraldehyde 3-phosphate, pyruvate, and lactate production (from steady state MS analyses - Fig. 2A–B).

Finally, PH-Fibs displayed alterations in redox homeostasis as indicated by increased amounts of reduced (GSH) and oxidized (GSSG) glutathione, evidence of utilization of the NADPH-generating pentose phosphate pathway and increased phosphogluconate and ribose phosphate (Fig. 2B, Suppl. Fig. 2B). These findings are consistent with our recent observations of oxygen-independent increased mitochondrial and cytoplasmic (NOX4 generated) ROS production in both human and bovine PH-Fibs[25].

To validate steady state observations suggesting increased uptake and oxidation of glucose through glycolysis, CO and PH-Fibs were cultured under normoxia in the presence of U-^{13}C-glucose for 5 min, 1, 8 and 24h. Tracing experiments via UHPLC-MS confirmed significantly increased ($p<0.05$ – ANOVA) glucose uptake, as well as intracellular and supernatant $^{13}C_{1\text{-}3}$-lactate generation in PH-Fibs as early as 8h from normoxic incubation with heavy glucose (Fig. 2C).

Nicotinamide adenine dinucleotide (NADH) concentrations are increased in PH Fibs

To determine if aerobic glycolysis in PH-Fibs formed the basis of increased concentrations of NADH (reflecting changes in the cellular redox status), FLIM (Fig. 3A, red color) and UHPLC-MS-based measurements (Fig. 3B) were used to visualize free-NADH and to directly measure NADH and NAD^+. Free NADH was markedly higher in bovine and human PH-Fibs relative to CO-Fibs (Fig. 3A). Direct measurements of total NADH and NAD^+ were performed through a targeted UHPLC-MS method, after determining linearity (Suppl. Fig. 4A) of the NADH detection down to a LOQ of 500 fmol injected, over four orders of magnitude. The results showed significant increased NADH in both bovine and human PH-Fibs compared to CO-Fibs (Fig. 3B). The NADH/NAD^+ ratio was also significantly increased in bovine PH-Fibs. The NADH/NAD^+ ratio was remarkably higher in each human PH-Fib population, but due to the extremely low NAD^+ value found in one human PH-Fib, the overall variability is high and the *P*-value is 0.07 (Suppl. Fig. 4B). To further validate these observations, we performed an orthogonal and frequently used measure of the NADH/NAD^+ ratio based on an enzymatic cycling reaction and represented by lactate/pyruvate ratio [26, 27] (Suppl. Fig. 4C).

Aerobic glycolysis and free NADH are critical in PH-Fib proliferation

We next determined if metabolic reprogramming and increased NADH concentrations were critical for promoting proliferation in PH-Fibs. Bovine and human PH-Fibs were treated with 2-deoxy-glucose (2-DG, 10mM) to block glucose metabolism, or with pyruvate (20mM), to directly decrease NADH by providing a substrate for NADH recycling to NAD^+ by lactate dehydrogenase. FLIM analysis showed both 2-DG and pyruvate decreased free-NADH in bovine and human PH-Fibs (Fig. 3C). Enzymatic cycling reaction measurement also demonstrated that 2-DG significantly decreased the NADH/NAD^+ ratio in bovine and human cells (Suppl. Fig. 4D). These decreases in free NADH resulted in a significant reduction in proliferation of both bovine and human PH-Fibs (Fig. 3D).

Aerobic glycolysis is critical for the pro-inflammatory PH-Fib phenotype

Recent reports demonstrate that pro-inflammatory activation of macrophages depends on metabolic reprogramming to aerobic glycolysis [28, 29]. Similar to observations in activated macrophages, we have previously reported that PH-Fibs express high amounts of pro-inflammatory mediators [5, 7]. Confirming our previous report of increased *MCP1* and *SDF1* gene and protein expression in PH-Fibs [7] we detected increased expression of MCP1 and SDF1 in vessels isolated by LCM of IPAH patients when compared to controls (Fig. 1B). Importantly, inhibition of aerobic glycolysis with 2-DG resulted in significantly attenuated transcription of MCP1 and SDF1 (Fig. 3E). Interestingly, recent reports have suggested that metabolic reprogramming to aerobic glycolysis prevents transcription of anti-inflammatory genes [28]. HOMX1 has been regarded as an important anti-inflammatory gene in PH [30, 31]. qPCR analysis from vessels isolated by LCM of IPAH patients showed decreased expression of the *HMOX1* relative to that in controls (Fig. 1B). Inhibition of aerobic glycolysis with 2-DG resulted in increased expression of *HMOX1* in both bovine and human PH-Fibs (Fig. 3E).

CtBP1 expression is increased in adventitial fibroblasts in pulmonary hypertension

Considering that aerobic glycolysis promotes increases in free NADH concentrations that in turn increase CtBP1 activity, we questioned whether CtBP1 expression was simultaneously increased in PH-Fibs. Notably, immunofluorescence and immuno-histochemical staining demonstrated that CtBP1 protein expression was increased *in situ* in the mouse and bovine hypoxic PH models as well as in pulmonary arteries from humans with IPAH relative to controls (Fig. 4A). Importantly, CtBP1 expression was primarily localized to the pulmonary arterial adventitia of hypoxic hypertensive subjects (Fig. 4A). Consistent with increased expression of CtBP1 in PH-Fibs observed in RNA-Seq analysis (p=0.033, FDR), expression of CtBP1 was increased in both cultured bovine and human PH-Fibs relative to CO-Fibs (Fig. 4B).

CtBP1 links aerobic glycolysis with proliferation in PH-Fibs

Simultaneous increases in CtBP1 expression and NADH accumulation suggest a functional role for CtBP1 in PH-Fibs. Therefore, we next determined the role of CtBP1 in PH-Fib proliferation using siRNA to knockdown *CTBP1* expression as well as using MTOB (2.5 mM) to inhibit CtBP1 activity. Both siCTBP1 and MTOB significantly inhibited PH-Fib proliferation (Fig. 5A). We also determined the effects of these agents on the expression of genes involved in cell proliferation and cell survival that had previously been shown to be direct targets of CtBP1 in cancer cells [15, 18, 24]. siCTBP1 and MTOB treatment resulted in significant upregulation of genes that promote growth arrest (e.g. cyclin-dependent kinase inhibitors genes, *P21* and *P15*) and apoptosis (e.g. *NOXA* and *PERP* - Fig. 5B, Suppl. Fig. 5).

The anti-proliferative effect induced by genetic or pharmacologic inhibition of CtBP1 was accompanied by a correction of the main metabolic aberrations of bovine and human PH-Fibs. Silencing of CTBP1 or treatment with MTOB resulted in a significant decrease in relative levels of metabolites involved in proliferative anabolic pathways (e.g. energy

metabolism; nucleotide biosynthesis, and antioxidant reactions) (Fig. 5C and E) and human PH-Fibs (Fig. 5D and F).

CtBP1 suppresses anti-inflammatory HMOX1 expression in PH-Fibs

Since metabolic reprogramming to aerobic glycolysis has been shown to suppress anti-inflammatory genes in macrophages [32], we hypothesized that disruption of CtBP1 signaling would increase transcription of anti-inflammatory genes in PH-Fibs. As mentioned above, the important anti-inflammatory gene implicated in the pathogenesis of PH, *HMOX1* [33–36], was decreased in IPAH vessels (Fig. 1B) and in PH-Fibs relative to controls (Fig. 6A). Consistent with the proposed repressive activity of CtBP1, siRNA knockdown or pharmacological inhibition of CtBP1 by MTOB resulted in significantly increased HMOX1 transcription (Fig. 6A).

These findings suggested that *HMOX1* was a direct target of the repressive activity of CtBP1, which to our knowledge had not been previously reported. We therefore used ChIP assay to determine direct binding of CtBP1 to the *HMOX1* promoter in human PH-Fibs. We also examined if 2-DG, pyruvate or MTOB would decrease recruitment of CtBP1 to the *HMOX1* promoter. *HMOX1* promoter binding was significantly higher in PH-Fibs compared to CO-Fibs. Knockdown of *CTBP1* by siRNA decreased binding of CtBP1 to the *HMOX1* promoter. 2-DG, Pyruvate and MTOB also suppressed binding of CtBP1 to *HMOX1* promoter region (Fig. 6B).

MTOB inhibits proliferation and inflammation in vivo in a mouse model of hypoxic PH

In light of the ability of MTOB to attenuate proliferation, correct metabolism and reduce inflammation of cultured PH-Fibs, we next sought to determine the therapeutic potential of MTOB *in vivo* in a mouse model of hypoxic PH (mice were chosen because the extremely high cost of the compound, e.g. cost of similar experiments in rats was calculated at over $35,000). Initial time course experiments using different time points of hypoxic exposure (4, 14 and 28 days) were performed to determine longitudinal expression of known genes involved in cellular proliferation and inflammatory activation demonstrated that expression of most of these genes peaked at day 4 (Suppl. Fig. 6A), which is consistent with previous studies in hypoxic mice [36, 37]. Hypoxic (4 days) whole mouse lung tissue exhibited increased glycolysis in comparison to normoxia as evidenced by the accumulation of lactate and increased NADH/NAD+ ratios (Fig. 7A, B). Metabolomics analyses by mass spectrometry indicated a progressive alteration of lung normoxic metabolic phenotype during prolonged exposure to hypoxia, alterations that were corrected by the MTOB treatment (Fig. 7C). Specifically, MTOB corrected the hypoxia-induced increase in glucose consumption and prevented the accumulation of glycolytic intermediates (glyceraldehyde 3-phosphate) and products (NADH/NAD^+ ratios – Fig. 7B and lactate – Fig. 7A, D). At day 4 of hypoxia, qPCR data demonstrated an 8-fold increase of expression of the pro-proliferative gene, cyclin-dependent kinase 1 (CDK1), which was inhibited by MTOB treatment (Fig. 8A). Immuno-staining for Ki67 nuclear proliferation-associated antigen revealed that at 4 days of hypoxia, the number of proliferating lung cells was significantly increased, and that MTOB treatment markedly decreased the number of proliferating cells (Fig. 8B). These changes were especially prominent in the distal pulmonary vasculature and in lung

parenchyma. Furthermore, qPCR analysis of the whole lung tissue demonstrated that hypoxia promoted monocyte chemotactic protein 1 (*Mcp1/Ccl2*) mRNA expression, and that MTOB treatment attenuated it (Fig. 8C). Correspondingly, we demonstrated an influx of monocytes/macrophages (expressing a macrophage marker, CD68) into pulmonary vascular adventitia of hypoxic hypertensive mice, and this pro-inflammatory response was markedly attenuated in distal pulmonary vasculature by MTOB treatment (Fig. 8D). Finally, to assess early pulmonary vascular remodeling (at day 4 of hypoxic exposure – before any significant deposition of collagen can be identified), we determined mRNA and protein expression of tenascin-C (TN-C), a matricellular protein whose expression is sharply upregulated in tissues undergoing remodeling, neovascularization, inflammation or tumorigenesis [38]. At day 4 of hypoxic exposure, TN-C mRNA expression in lung tissues was upregulated 4-fold as compared to normoxic controls and TN-C protein was prominent in distal pulmonary vasculature (Fig. 8E, F). MTOB treatment attenuated TN-C expression at mRNA and protein (Fig. 8E, F) levels. We did not observe significant difference of CDK1, TN-C and MCP1 mRNA level between untreated and MTOB (1g/kg) treated normoxic mice (Suppl. Fig. 6B). H&E and alpha smooth muscle actin (α-SMA) staining also showed perivascular inflammation and vascular remodeling, respectively, in hypoxic mice lung tissue and both were attenuated by MTOB treatment (Suppl. Fig. 7).

Taken together, MTOB treatment of hypoxic hypertensive mice successfully attenuated pulmonary vascular cell proliferation, inflammation (as seen by the reduction in *Ccl2/Mcp1* expression and decreased recruitment of CD68-expressing macrophages) and vascular remodeling (TN-C, α-SMA and H&E staining).

Discussion

In the present study we have demonstrated that in the pathogenesis of pulmonary hypertension adventitial fibroblasts undergo metabolic reprogramming with increased aerobic glycolysis relative to oxidative phosphorylation. Our findings expand upon our previous observations of anomalous mitochondrial metabolism in pulmonary hypertension, and highlight the critical function of metabolic adaptations in supporting fibroblast proliferation and inflammatory activation [25]. We have also demonstrated increased expression of CtBP1 in the lungs of hypoxia-induced experimental PH in the cow and mouse model, as well as in IPAH patients and linked that expression to disease pathogenesis. Importantly, we identified CtBP1, a transcriptional co-repressor that is activated by increased free-NADH secondary to glycolytic reprogramming, as a molecular link and potential therapeutic target to correct the aberrant metabolic, hyper-proliferative and inflammatory phenotype of bovine and human PH-Fibs *in vitro* and in hypoxic mice *in vivo*. Our study thereby supports the novel hypothesis that chronic hypoxic PH and seemingly IPAH or familial pulmonary arterial hypertension (fPAH) leads to the rewiring of cellular metabolic programs that utilize alterations in the cellular redox state (i.e. available NADH) to control activity of CtBP1, and thus coordinate expression of a network of genes implicated in cell proliferation, apoptosis resistance and inflammation (Fig. 8G).

PH pathology often involves an imbalance of cell proliferation versus cell death and thus the hypothesis has been put forth that the cellular and molecular features seen in PH resemble

hallmark characteristics described for cancer [11, 12, 39]. Changes in metabolism have emerged as key contributors to cancer pathophysiology and inflammation and thus have become emerging targets for novel diagnostic and therapeutic approaches that may have relevance to pulmonary hypertension [11, 39, 40]. Our study provides strong evidence that *in vivo* and *in vitro* aerobic glycolysis is a metabolic adaptation in pulmonary artery adventitial fibroblasts in the setting of chronic hypoxia as well as in IPAH. Metabolic data here suggest that, akin to Warburg metabolism in cancer cells and inflammatory macrophages, incomplete glucose oxidation affords PH-Fibs with building blocks to support anabolic reactions (amino acid anabolism, fatty acid synthesis, urea cycle, gluconeogenesis) necessary to sustain proliferation and inflammatory activation, counteract oxidative stress and promote resistance to apoptosis.

Unlike other transcriptional co-repressors, CtBP1 is uniquely structured to sense increases in free NADH concentrations which typically occur secondary to glycolytic reprogramming [22, 23]. Studies by our group and others have demonstrated that changes in the cellular reducing environment alter the interaction of CtBP1 with DNA-binding transcriptional repressors [23, 27, 41, 42]. As a ‘foe ‘of multiple tumor suppressors, CtBP1 also provides a link between transcriptional regulation and the metabolic status of the cell [15]. In line with the hypothesis that free NADH concentrations increased CtBP activity, treatment of PH-Fibs with 2-DG or pyruvate to interfere with aerobic glycolysis and promote NADH oxidation to NAD^+ in PH-Fibs, respectively, was associated with attenuation of activity of CtBP1. Decreased CtBP1 activity translated into reduced PH-Fibs proliferation and attenuated inflammatory activation, normalization of aberrant metabolic phenotypes and increased expression of anti-inflammatory *HMOX1*. In PH-Fibs (both bovine and human) this increase in CtBP1 activity was maintained in the absence of a hypoxic stimulus indicating that akin to what has been described in cancer cells, stable rewiring or reprogramming of metabolism occurs in PH-Fibs and drives activity of transcriptional repressors, such as CtBP1. Strikingly, knockdown of *CTBP1* by siRNA or inhibition of CtBP1 dehydrogenase activity by MTOB treatment attenuated proliferation of PH-Fibs (Fig. 5A). Similar to cancer cells, inhibition of CtBP1 increased expression of cyclin-dependent kinase inhibitors (p15 and p21) and pro-apoptotic genes (NOXA and PERP) [18, 23].

Our findings regarding an important role for CtBP1 mediated change in cell phenotype in PH are consistent with previous findings in PH. It was recently reported that hypoxia, a paramount stimulus for the development of pulmonary hypertension, suppresses the expression of inhibitor of differentiation 1 (Id1), a downstream target of the BMPR2 pathway, in human pulmonary artery smooth muscle cells (HPASMC) [43]. Hypoxia-induced changes in the $NADH/NAD^+$ ratio and histone deacetylases (HDACs) upregulated transcriptional co-repressor CtBP-1 activity and subsequently attenuated BMP signaling [43]. Due to the near universal association between metabolic reprogramming and an activated cell phenotype in both cancer and PH, there has been great interest in identifying factors that might link these changes. CtBPs have emerged as candidates in this regard. Importantly, we also observed significantly reduced levels of Id1 and Id2 in PH-Fibs with high CtBP1 expression (Table 2). These findings are furthermore consistent with the proposed role of CtBPs in tumor genesis and tumor progression as we observe similar CtBP1 targets including p15, p21, NOXA, and PERP [15, 18, 24].

Inflammation is critically involved in the pathogenesis of PH though how this is related to or regulated by metabolic reprogramming is unclear [39]. Because of its prominent role in the pathogenesis of PH, we focused attention on the anti-inflammatory gene *HMOX1* and demonstrated that inhibition of aerobic glycolysis was associated with robust increases in *HMOX1* expression. The results showed that *HMOX1* is a direct target of CtBP1, which has not previously been reported. Heme oxygenase (HO) catalyzes the oxidation of heme to carbon monoxide and biliverdin, which is then converted to bilirubin by biliverdin reductase [44]. Carbon monoxide released by HO-1 confers protection against vasoconstriction and vascular remodeling induced by hypoxia *in vitro* [45, 46]. Studies using an HO-1 null mouse model suggest HO-1 plays a central role in protecting the right ventricle from hypoxic pulmonary pressure-induced injury [47]. Conversely, transgenic mice with constitutive, lung-specific overexpression of HO-1 do not manifest the early inflammatory changes and are protected from PH on continued exposure to hypoxia [30], suggesting increasing HO-1 can serve as a prevention or therapeutic intervention for PH. Collectively, our findings suggest it is possible that targeting CtBP1 has the potential to convert pro-inflammatory activation to an anti-inflammatory phenotype and thus to suppress inflammation and vascular remodeling as was observed in our MTOB treated hypoxic mice.

Until recently CtBP1 had been implicated in responding to the metabolic status of the cell rather than regulating the cellular metabolic pathways [18, 48]. Interestingly, a recent study demonstrated that CtBP promotes glutaminolysis in cancer cells by directly decreasing SIRT4 gene expression, a mitochondrial repressor of glutamate dehydrogenase and thus glutaminolysis. Therefore, increased CtBP levels in cancer cells repress SIRT4, which in turn leads to an increase in glutamine supply that promotes ammonia production to neutralize the acidification associated with increased glycolytic fluxes [49]. Since glycolytic rate drops as pH falls, the role of CtBP1 in preventing intracellular acidification sustains glycolysis and, in turn, cancer cell growth. RNA-Seq and metabolomic analysis from our study are consistent with these findings, showing higher level of glutamate dehydrogenase (p=0.02, FDR) together with significantly decreased SIRT4 level (Table 2) in PH-Fibs, concomitantly with increases in the expression and activation of CtBP1. Consistently, inhibition of CtBP1 by siRNA or MTOB corrected the metabolic phenotype of PH-Fibs and mouse lung tissue (Fig. 5C–F, Fig. 7C–D). In particular, MTOB treatment prevented the accumulation of glycolytic reprogramming induced by prolonged exposure to hypoxia in mouse lungs (Fig. 7C). Indeed, while prolonged hypoxia promoted increases in glycolysis in mice lungs, MTOB treatment resulted in normoxic-like levels of glyceraldehyde 3-phosphate, lactate and NADH/NAD+ ratios (Fig. 7). Thus, like cancer, the proliferation promoting function of CtBP1 in PH-Fibs requires its involvement in metabolic control. We have previously reported that the PH-Fibs described in this study fail to exhibit high expression levels of α-SMA and Col1 and in fact continue to express markers of mesenchymal progenitors such as RGS5 (Table 2). CtBP1 could thus be an essential regulator to support self-renewal and expansion particularly in hypoxic environments as might be observed at the medial-adventitial border of inflamed vessels. Of note, metabolic reprogramming towards aerobic glycolysis was observed in PH-Fibs cultured under normoxia, suggesting that whether hypoxia represents a key trigger to promote metabolic reprogramming and CtBP1 activation, hypoxia-independent perpetuation of the metabolic

reprogramming-CtBP1 activity axis results in a feed-forward mechanism that can be disrupted by pharmacological or genetic ablation of either component of the axis *in vitro* and *in vivo*.

Finally, our *ex vivo* data demonstrate that targeting CtBP1 at the RNA level via siRNA or at activity level by MTOB, or reducing NADH level by 2-DG or pyruvate can inhibit the proliferative and augment the anti-inflammatory phenotype of PH-Fibs. These results provide evidence that small molecules such as MTOB or NSC9539 (a CDC25 inhibitor that inhibits CtBP1-EIA interaction) that demonstrate anti-cancer properties may be used as a treatment tools to treat hypoxia-induced PH [50, 51]. As a first step in examining this hypothesis we treated mice made hypoxic with MTOB (at present a prohibitively expensive drug). We found MTOB successfully attenuated vascular remodeling (cell proliferation, glycolytic and overall metabolic reprogramming, macrophage accumulation, and extracellular matrix production) induced by hypoxia. Thus, it is tempting to speculate that in certain forms or stages of PH, including hypoxia (Group #3) targeting the transcriptional repressor CtBP1, which links changes in metabolism to an activated cell phenotype may have beneficial effects.

Supplementary Material

Refer to Web version on PubMed Central for supplementary material.

Acknowledgments

We dedicate this work to the memory of our colleague, Dr. QingHong Zhang, an inquisitive scientist and joyful spirit who initiated our work with CtBP1 but who passed away prior to the publication of this article. Dr. Zhang leaves behind an excellent body of scholarship focusing on the role of CtBP1 in the cancer field. We are deeply saddened by her loss and dedicate this work to her. The authors are thankful to Marcia McGowan for her outstanding help in preparing the manuscript; Dr. Dale Brown and Andy Poczobutt for coordinating the calf studies; and Alma Islas-Trejo for making the libraries for RNA-Seq.

Funding Sources: This manuscript was supported by National Institutes of Health grants NIH HL084923, HL014985, HL114887; Department of Defense Grant DoD #W81XWH-15-1-0280; KONTAKT grant LH 11055 and LH 15071; and John E. Rouse Endowment for Animal Breeding Research, Colorado State University.

References

1. Simonneau G, Gatzoulis MA, Adatia I, Celermajer D, Denton C, Ghofrani A, Gomez Sanchez MA, Krishna Kumar R, Landzberg M, Machado RF, Olschewski H, Robbins IM, Souza R. Updated clinical classification of pulmonary hypertension. J Am Coll Cardiol. 2013; 62:D34–41. [PubMed: 24355639]
2. Price LC, Wort SJ, Perros F, Dorfmuller P, Huertas A, Montani D, Cohen-Kaminsky S, Humbert M. Inflammation in pulmonary arterial hypertension. Chest. 2012; 141:210–21. [PubMed: 22215829]
3. Stenmark KR, Meyrick B, Galie N, Mooi WJ, McMurtry IF. Animal models of pulmonary arterial hypertension: the hope for etiological discovery and pharmacological cure. Am J Physiol Lung Cell Mol Physiol. 2009; 297:L1013–1032. [PubMed: 19748998]
4. Das M, Burns N, Wilson SJ, Zawada WM, Stenmark KR. Hypoxia exposure induces the emergence of fibroblasts lacking replication repressor signals of PKCzeta in the pulmonary artery adventitia. Cardiovasc Res. 2008; 78:440–448. [PubMed: 18218684]
5. El Kasmi KC, Pugliese SC, Riddle SR, Poth JM, Anderson AL, Frid MG, Li M, Pullamsetti SS, Savai R, Nagel MA, Fini MA, Graham BB, Tuder RM, Friedman JE, Eltzschig HK, Sokol RJ,

Stenmark KR. Adventitial fibroblasts induce a distinct proinflammatory/profibrotic macrophage phenotype in pulmonary hypertension. J Immunol. 2014; 193:597–609. [PubMed: 24928992]

6. Krick S, Hanze J, Eul B, Savai R, Seay U, Grimminger F, Lohmeyer J, Klepetko W, Seeger W, Rose F. Hypoxia-driven proliferation of human pulmonary artery fibroblasts: cross-talk between HIF-1alpha and an autocrine angiotensin system. FASEB J. 2005; 19:857–859. [PubMed: 15718424]
7. Li M, Riddle SR, Frid MG, El Kasmi KC, McKinsey TA, Sokol RJ, Strassheim D, Meyrick B, Yeager ME, Flockton AR, McKeon BA, Lemon DD, Horn TR, Anwar A, Barajas C, Stenmark KR. Emergence of fibroblasts with a proinflammatory epigenetically altered phenotype in severe hypoxic pulmonary hypertension. J Immunol. 2011; 187:2711–22. [PubMed: 21813768]
8. Panzhinskiy E, Zawada WM, Stenmark KR, Das M. Hypoxia induces unique proliferative response in adventitial fibroblasts by activating PDGFbeta receptor-JNK1 signalling. Cardiovasc Res. 2012; 95:356–365. [PubMed: 22735370]
9. Wang D, Zhang H, Li M, Frid MG, Flockton AR, McKeon BA, Yeager ME, Fini MA, Morrell NW, Pullamsetti SS, Velegala S, Seeger W, McKinsey TA, Sucharov CC, Stenmark KR. MicroRNA-124 controls the proliferative, migratory, and inflammatory phenotype of pulmonary vascular fibroblasts. Circ Res. 2014; 114:67–78. [PubMed: 24122720]
10. Guignabert C, Tu L, Le Hiress M, Ricard N, Sattler C, Seferian A, Huertas A, Humbert M, Montani D. Pathogenesis of pulmonary arterial hypertension: lessons from cancer. Eur Respir Rev. 2013; 22:543–551. [PubMed: 24293470]
11. Hanahan D, Weinberg RA. Hallmarks of cancer: the next generation. Cell. 2011; 144:646–674. [PubMed: 21376230]
12. Paulin R, Michelakis ED. The metabolic theory of pulmonary arterial hypertension. Circ Res. 2014; 115:148–164. [PubMed: 24951764]
13. Vander Heiden MG, Cantley LC, Thompson CB. Understanding the Warburg effect: the metabolic requirements of cell proliferation. Science. 2009; 324:1029–1033. [PubMed: 19460998]
14. Zhao L, Ashek A, Wang L, Fang W, Dabral S, Dubois O, Cupitt J, Pullamsetti SS, Cotroneo E, Jones H, Tomasi G, Nguyen QD, Aboagye EO, El-Bahrawy MA, Barnes G, Howard LS, Gibbs JS, Gsell W, He JG, Wilkins MR. Heterogeneity in lung (18)FDG uptake in pulmonary arterial hypertension: potential of dynamic (18)FDG positron emission tomography with kinetic analysis as a bridging biomarker for pulmonary vascular remodeling targeted treatments. Circulation. 2013; 128:1214–1224. [PubMed: 23900048]
15. Chinnadurai G. The transcriptional corepressor CtBP: a foe of multiple tumor suppressors. CancerRes. 2009; 69:731–734.
16. Pena C, Garcia JM, Garcia V, Silva J, Dominguez G, Rodriguez R, Maximiano C, Garcia de Herreros A, Munoz A, Bonilla F. The expression levels of the transcriptional regulators p300 and CtBP modulate the correlations between SNAIL, ZEB1, E-cadherin and vitamin D receptor in human colon carcinomas. Int J Cancer. 2006; 119:2098–2104. [PubMed: 16804902]
17. Wang R, Asangani IA, Chakravarthi BV, Ateeq B, Lonigro RJ, Cao Q, Mani RS, Camacho DF, McGregor N, Schumann TE, Jing X, Menawat R, Tomlins SA, Zheng H, Otte AP, Mehra R, Siddiqui J, Dhanasekaran SM, Nyati MK, Pienta KJ, Palanisamy N, Kunju LP, Rubin MA, Chinnaiyan AM, Varambally S. Role of transcriptional corepressor CtBP1 in prostate cancer progression. Neoplasia. 2012; 14:905–914. [PubMed: 23097625]
18. Di LJ, Byun JS, Wong MM, Wakano C, Taylor T, Bilke S, Baek S, Hunter K, Yang H, Lee M, Zvosec C, Khramtsova G, Cheng F, Perou CM, Miller CR, Raab R, Olopade OI, Gardner K. Genome-wide profiles of CtBP link metabolism with genome stability and epithelial reprogramming in breast cancer. Nat Commun. 2013; 4:1449. [PubMed: 23385593]
19. Grooteclaes M, Deveraux Q, Hildebrand J, Zhang Q, Goodman RH, Frisch SM. C-terminal-binding protein corepresses epithelial and proapoptotic gene expression programs. Proc Natl Acad Sci U S A. 2003; 100:4568–4573. [PubMed: 12676992]
20. Zhang G, Yan Y, Kang L, Cao Q, Ke K, Wu X, Gao Y, Hang Q, Li C, Zhu L, Yuan Q, Wu Q, Cheng C. Involvement of CtBP2 in LPS-induced microglial activation. J Mol Histol. 2012; 43:327–334. [PubMed: 22426895]

21. Byun JS, Gardner K. C-Terminal Binding Protein: A Molecular Link between Metabolic Imbalance and Epigenetic Regulation in Breast Cancer. Int J Cell Biol. 2013; 2013:647975. [PubMed: 23762064]
22. Fjeld CC, Birdsong WT, Goodman RH. Differential binding of NAD+ and NADH allows the transcriptional corepressor carboxyl-terminal binding protein to serve as a metabolic sensor. Proc Natl Acad Sci U S A. 2003; 100:9202–9207. [PubMed: 12872005]
23. Zhang Q, Piston DW, Goodman RH. Regulation of corepressor function by nuclear NADH. Science. 2002; 295:1895–7. [PubMed: 11847309]
24. Straza MW, Paliwal S, Kovi RC, Rajeshkumar B, Trenh P, Parker D, Whalen GF, Lyle S, Schiffer CA, Grossman SR. Therapeutic targeting of C-terminal binding protein in human cancer. Cell Cycle. 2010; 9:3740–3750. [PubMed: 20930544]
25. Plecita-Hlavata L, Tauber J, Li M, Zhang H, Flockton AR, Pullamsetti SS, Chelladurai P, D'Alessandro A, El Kasmi KC, Jezek P, Stenmark KR. Constitutive Reprogramming of Fibroblast Mitochondrial Metabolism in Pulmonary Hypertension. Am J Respir Cell Mol Biol. 2016; 55:47–57. [PubMed: 26699943]
26. Williamson DH, Lund P, Krebs HA. The redox state of free nicotinamide-adenine dinucleotide in the cytoplasm and mitochondria of rat liver. Biochem J. 1967; 103:514–527. [PubMed: 4291787]
27. Zhang Q, Yoshimatsu Y, Hildebrand J, Frisch SM, Goodman RH. Homeodomain interacting protein kinase 2 promotes apoptosis by downregulating the transcriptional corepressor CtBP. Cell. 2003; 115:177–186. [PubMed: 14567915]
28. Kelly B, O'Neill LA. Metabolic reprogramming in macrophages and dendritic cells in innate immunity. Cell Res. 2015; 25:771–784. [PubMed: 26045163]
29. Stenmark KR, Tuder RM, El Kasmi KC. Metabolic reprogramming and inflammation act in concert to control vascular remodeling in hypoxic pulmonary hypertension. J Appl Physiol. 2015; 119:1164–72. [PubMed: 25930027]
30. Minamino T, Christou H, Hsieh CM, Liu Y, Dhawan V, Abraham NG, Perrella MA, Mitsialis SA, Kourembanas S. Targeted expression of heme oxygenase-1 prevents the pulmonary inflammatory and vascular responses to hypoxia. Proc Natl Acad Sci U S A. 2001; 98:8798–8803. [PubMed: 11447290]
31. Palsson-McDermott EM, O'Neill LA. The Warburg effect then and now: from cancer to inflammatory diseases. Bioessays. 2013; 35:965–973. [PubMed: 24115022]
32. Palsson-McDermott EM, Curtis AM, Goel G, Lauterbach MA, Sheedy FJ, Gleeson LE, van den Bosch MW, Quinn SR, Domingo-Fernandez R, Johnston DG, Jiang JK, Israelsen WJ, Keane J, Thomas C, Clish C, Vander Heiden M, Xavier RJ, O'Neill LA. Pyruvate kinase M2 regulates Hif-1alpha activity and IL-1beta induction and is a critical determinant of the warburg effect in LPS-activated macrophages. Cell Metab. 2015; 21:65–80. [PubMed: 25565206]
33. Belhaj A, Dewachter L, Kerbaul F, Brimioulle S, Dewachter C, Naeije R, Rondelet B. Heme oxygenase-1 and inflammation in experimental right ventricular failure on prolonged overcirculation-induced pulmonary hypertension. PloS One. 2013; 8:e69470. [PubMed: 23936023]
34. Constantin M, Choi AJ, Cloonan SM, Ryter SW. Therapeutic potential of heme oxygenase-1/carbon monoxide in lung disease. Int J Hypertens. 2012; 2012:859235. [PubMed: 22518295]
35. Liang OD, Mitsialis SA, Chang MS, Vergadi E, Lee C, Aslam M, Fernandez-Gonzalez A, Liu X, Baveja R, Kourembanas S. Mesenchymal stromal cells expressing heme oxygenase-1 reverse pulmonary hypertension. Stem Cells. 2011; 29:99–107. [PubMed: 20957739]
36. Vergadi E, Chang MS, Lee C, Liang OD, Liu X, Fernandez-Gonzalez A, Mitsialis SA, Kourembanas S. Early macrophage recruitment and alternative activation are critical for the later development of hypoxia-induced pulmonary hypertension. Circulation. 2011; 123:1986–1995. [PubMed: 21518986]
37. Paddenberg R, Stieger P, von Lilien AL, Faulhammer P, Goldenberg A, Tillmanns HH, Kummer W, Braun-Dullaeus RC. Rapamycin attenuates hypoxia-induced pulmonary vascular remodeling and right ventricular hypertrophy in mice. Respir Res. 2007; 8:15. [PubMed: 17319968]
38. Hsia HC, Schwarzbauer JE. Meet the tenascins: multifunctional and mysterious. J Biol Chem. 2005; 280:26641–26614. [PubMed: 15932878]

39. Tuder RM, Archer SL, Dorfmuller P, Erzurum SC, Guignabert C, Michelakis E, Rabinovitch M, Schermuly R, Stenmark KR, Morrell NW. Relevant issues in the pathology and pathobiology of pulmonary hypertension. J Am Coll Cardiol. 2013; 62:D4–12. [PubMed: 24355640]
40. Tennant DA, Duran RV, Gottlieb E. Targeting metabolic transformation for cancer therapy. Nat Rev Cancer. 2010; 10:267–277. [PubMed: 20300106]
41. Kim JH, Cho EJ, Kim ST, Youn HD. CtBP represses p300-mediated transcriptional activation by direct association with its bromodomain. Nat Struct Mol Biol. 2005; 12:423–428. [PubMed: 15834423]
42. Mirnezami AH, Campbell SJ, Darley M, Primrose JN, Johnson PW, Blaydes JP. Hdm2 recruits a hypoxia-sensitive corepressor to negatively regulate p53-dependent transcription. Curr Biol. 2003; 13:1234–1239. [PubMed: 12867035]
43. Wu X, Chang MS, Mitsialis SA, Kourembanas S. Hypoxia regulates bone morphogenetic protein signaling through C-terminal-binding protein 1. Circ Res. 2006; 99:240–247. [PubMed: 16840720]
44. Abraham NG, Levere RD, Lin JH, Beru N, Hermine O, Goldwasser E. Co-regulation of heme oxygenase and erythropoietin genes. J Cell Biochem. 1991; 47:43–48. [PubMed: 1939365]
45. Morita T, Mitsialis SA, Koike H, Liu Y, Kourembanas S. Carbon monoxide controls the proliferation of hypoxic vascular smooth muscle cells. J Biol Chem. 1997; 272:32804–32809. [PubMed: 9407056]
46. Morita T, Perrella MA, Lee ME, Kourembanas S. Smooth muscle cell-derived carbon monoxide is a regulator of vascular cGMP. Proc Natl Acad Sci U S A. 1995; 92:1475–1479. [PubMed: 7878003]
47. Yet SF, Perrella MA, Layne MD, Hsieh CM, Maemura K, Kobzik L, Wiesel P, Christou H, Kourembanas S, Lee ME. Hypoxia induces severe right ventricular dilatation and infarction in heme oxygenase-1 null mice. J Clin Invest. 1999; 103:R23–29. [PubMed: 10207174]
48. Di LJ, Fernandez AG, De Siervi A, Longo DL, Gardner K. Transcriptional regulation of BRCA1 expression by a metabolic switch. Nat Struct Mol Biol. 2010; 17:1406–1413. [PubMed: 21102443]
49. Wang L, Zhou H, Wang Y, Cui G, Di LJ. CtBP maintains cancer cell growth and metabolic homeostasis via regulating SIRT4. Cell Death Dis. 2015; 6:e1620. [PubMed: 25633289]
50. Blevins MA, Kouznetsova J, Krueger AB, King R, Griner LM, Hu X, Southall N, Marugan JJ, Zhang Q, Ferrer M, Zhao R. Small Molecule, NSC95397, Inhibits the CtBP1-Protein Partner Interaction and CtBP1-Mediated Transcriptional Repression. J Biomol Screen. 2015; 20:663–672. [PubMed: 25477201]
51. Yang Y, Yang WS, Yu T, Yi YS, Park JG, Jeong D, Kim JH, Oh JS, Yoon K, Kim JH, Cho JY. Novel anti-inflammatory function of NSC95397 by the suppression of multiple kinases. Biochem Pharmacol. 2014; 88:201–215. [PubMed: 24468133]

Clinical Perspective

What Is New?

- In pulmonary hypertension (PH), little is known regarding the molecular mechanisms that link the metabolic state of cells to gene transcription and functional changes in their phenotype. We show that C-terminal binding protein1 (CtBP1), a transcription factor that is activated by increased free NADH, acts as a molecular “linker” to drive the proliferative and pro-inflammatory phenotype of adventitial fibroblasts within the hypertensive vessel wall.
- This work supports the novel hypothesis that some forms of PH lead to the re-wiring of cellular metabolic programs that utilize alterations in the cellular redox state to control the activity of CtBP1, which then coordinates expression of a network of genes implicated in cell proliferation, apoptosis resistance, and inflammation.

Clinical Implications

- We also found that treatment of fibroblasts from the pulmonary hypertensive vessel and of hypoxic mice with a pharmacologic inhibitor of CtBP1, 4-methylthio-2-oxybutyric acid (MTOB) lead to a normalization of proliferation, inflammation, and the aberrant metabolic signaling.
- Our results suggest that targeting this metabolic sensor may be a more specific approach to treating metabolic abnormalities in PH than use of more global metabolic inhibitors.
- It will be important in future studies to determine if inhibition of CtBP1 can be combined with other vasodilating drugs to effect reversal of established severe forms of PH.

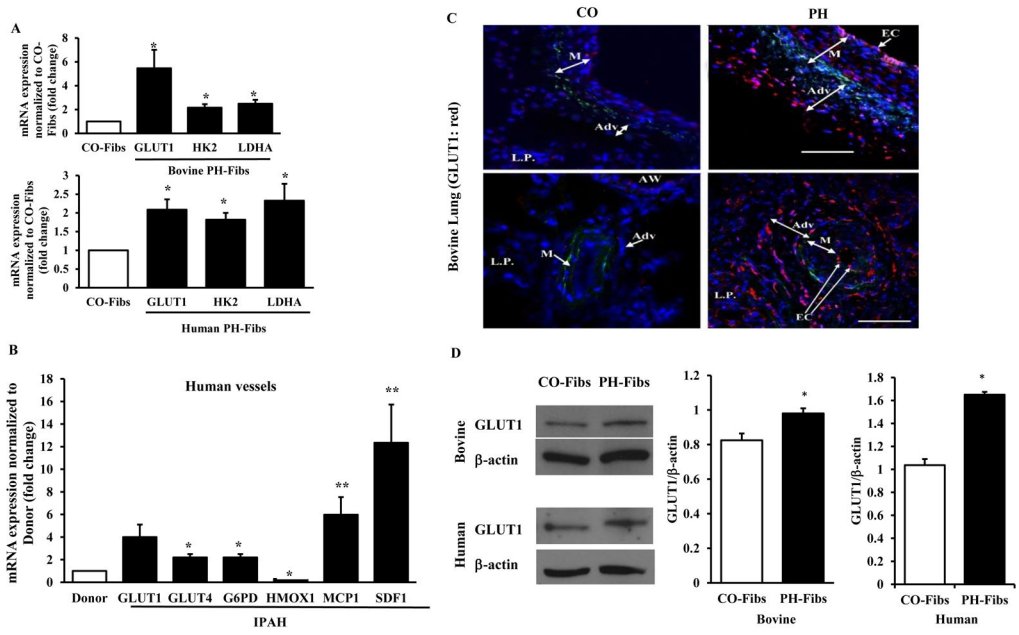

Figure 1.

Bovine and human hypoxic-induced hypertensive pulmonary artery adventitial fibroblast cells (PH-Fibs) exhibit differences in mRNA and protein expression of genes involved in glucose metabolism compared to control fibroblasts (CO-Fibs). (A) qPCR showed significantly higher expression of glucose transporter 1 (*GLUT1*), hexokinase 2 (*HK2*) and lactate dehydrogenase A (*LDHA*) mRNA level in both bovine and human PH-Fibs compared to CO-Fibs. (B) Up-regulation of *GLUT1, GLUT4, Glucose-6-phosphate dehydrogenase (G6PD), monocyte chemotactic protein 1(MCP1), stromal cell-derived factor1 (SDF1),* and down-regulation of *heme oxygenase-1 (HMOX1)* were observed in vessels isolated by LCM of IPAH patients compared to controls. (C) Immunofluorescent staining showed higher expression of GLUT1 (red color) in the adventitia of chronic hypoxia-induced pulmonary hypertensive bovine lung section compared to control lungs. (L.P: lung parenchyma; AW: airway; EC: endothelium; M: media; Adv: adventitia. Scale bar=100μM). (D) Western blot confirmed higher protein expression of GLUT1 in both bovine and human PH-Fibs. (Data was presented as mean ± sem, n=3–9; *, $P<0.05$, **, $P<0.01$, compared to CO-Fibs or vessels from human donors).

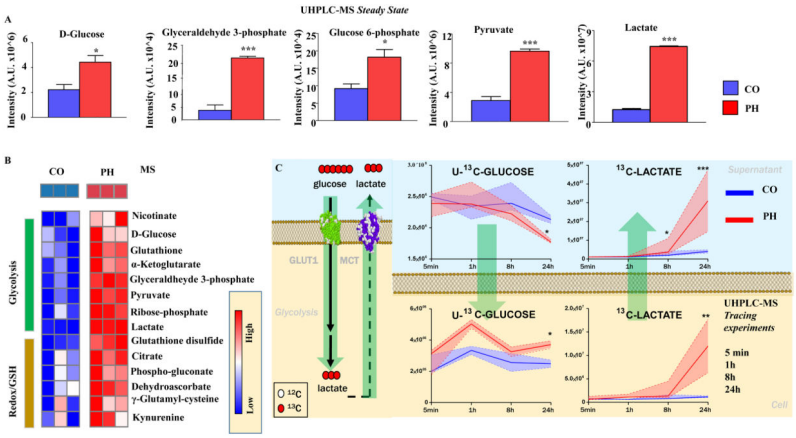

Figure 2.

Metabolomics evidence for aerobic glycolysis in PH-Fibs. Steady-state and flux tracing experiments were performed via Ultra-High Pressure Liquid Chromatography-Mass Spectrometry (UHPLC-MS) by incubating bovine CO and PH-Fibs with U-^{13}C-glucose. (A) Steady state UHPLC- MS demonstrated increased glucose content, utilization through glycolysis and increased lactate production in PH-Fibs compared to CO-Fibs (n=3, *, P<0.05, ***, P<0.001, compared to CO-Fibs). (B) Heat-map generated from MS showed differences in metabolite production between CO-Fibs and PH-Fibs. Each column represents an individual samples from each group, and the differences between each groups are significantly different (P < 0.05). (C) Tracing experiments were performed by incubating CO and PH-Fibs (n=3) for 5 min, 1, 8 or 24h with U-^{13}C-glucose to confirm increased uptake and catabolism of glucose through aerobic glycolysis in PH-Fibs cultured in normoxia. Median (continuous line) and interquartile ranges (dashed lines) are shown for control (CO - blue) and PH-Fibs (PH - red) (*, P < 0.05, **, P < 0.01, ***, P < 0.001 compared to CO-Fibs-repeated measures ANOVA).

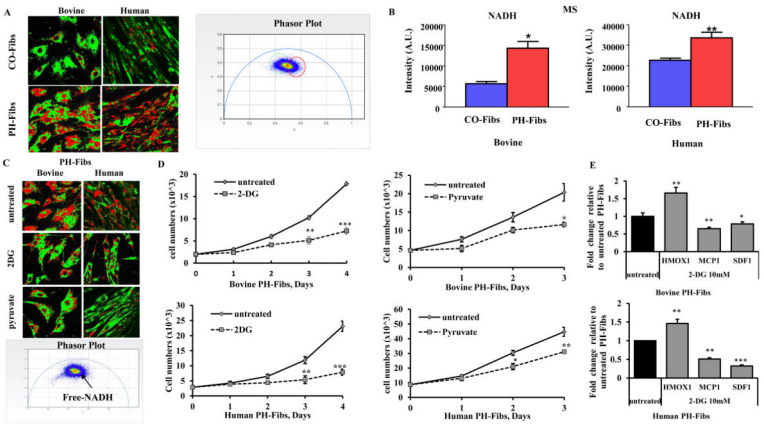

Figure 3.

PH-Fibs exhibit increased NADH levels compared to CO-Fibs. 2-deoxy-glucose (2DG) and pyruvate inhibited proliferation and attenuated the inflammatory phenotype of PH-Fibs by decreasing NADH levels and thus decreasing CtBP1 activity. (A) Fluorescence lifetime imaging (FLIM) of two-photon excited NADH was performed to directly visualize free-NADH (shorter lifetime, red color). Phasor plot showed free-NADH collection localization (red circle). A remarkably increased detection of free-NADH was seen in PH-Fibs compared to CO-Fibs. (B) Direct NADH measurements were performed through a targeted UHPLC-MS method, after determining linearity of the NADH detection down to a LOQ of 500 fmol injected, over four orders of magnitude. NADH analysis of bovine and human via UHPLC-MS confirmed the results obtained with FLIM and showed significant increase of NADH in PH-Fibs compared to CO-Fibs (n=3, *, P<0.05, **, P<0.01 compared to CO-Fibs). (C) Treatment with 2DG (10mM) and pyruvate (20mM) for 48hrs decreased free-NADH (red color) dectection (FLIM) in PH-Fibs. (D) 2DG and pyruvate significantly inhibited proliferation of PH-Fibs. (n=3, *, P < 0.05, **, P < 0.01, ***, P < 0.001 compared to untreated PH-Fibs-repeated measures ANOVA). (E) 2DG decreased pro-inflammatory factors (MCP1, SDF1), and increased anti-inflammatory factor (*HMOX1*) expression in PH-Fibs. (n=3–8. *, P < 0.05, **, P < 0.01, ***, P < 0.001 compared to untreated PH-Fibs).

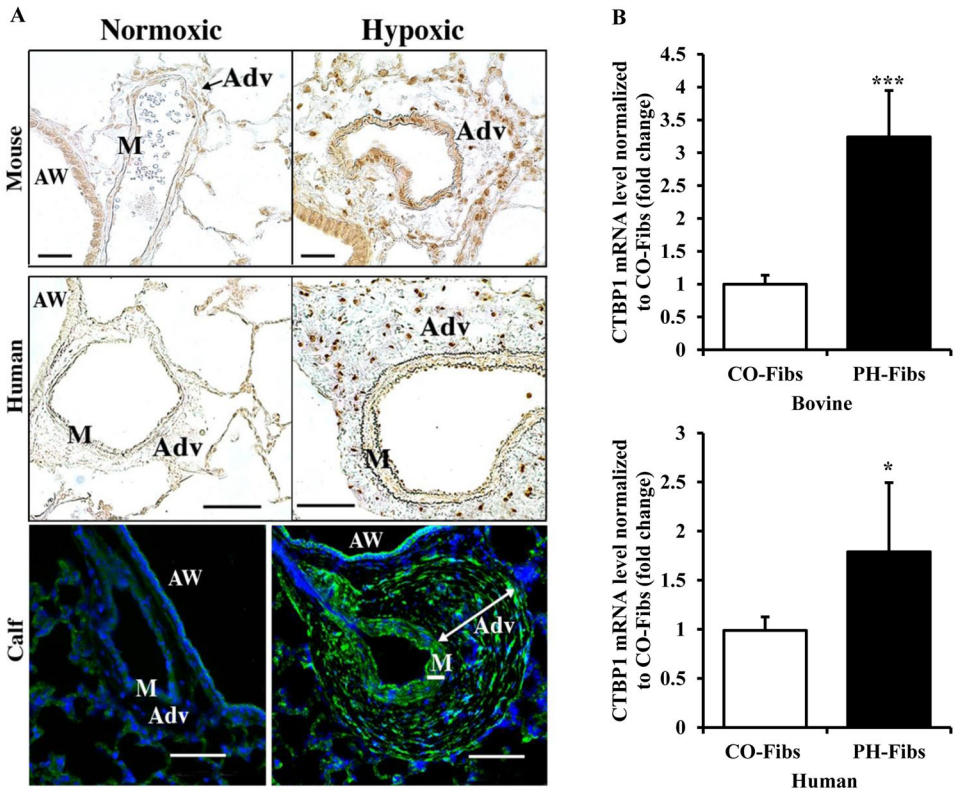

Figure 4.

CtBP1 expression is increased in the adventitia of hypertensive pulmonary arteries and in isolated hypertensive adventitial fibroblast cells. (A) Immunohistochemistry (dark brown staining) and immunofluorescent staining (green staining, space bar=100um) showed that CtBP1 protein is overexpressed in the adventitia of chronic hypoxia-induced pulmonary hypertensive, but not control, mouse, human and bovine PA (AW: airway, M: media, Adv: adventitia). (B) Real-time PCR data showed that high CtBP1 expression is maintained under normoxia conditions in fibroblasts cultured from both hypertensive calves and humans with IPAH. (n=4–15. *, $P < 0.05$, ***, $P < 0.001$ compared to CO-Fibs).

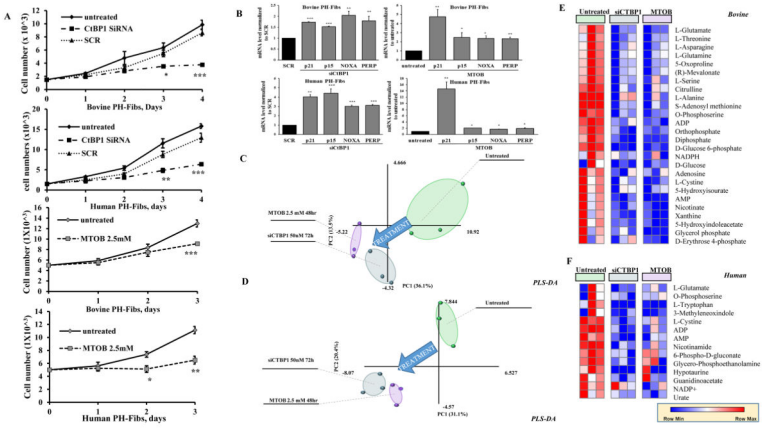

Figure 5.

CtBP1 regulates the expression of genes involved in proliferation, cell survival and metabolic state in adventitial fibroblasts. Inhibition of CtBP1 by siRNA (50nM, 72hrs) or by MTOB (2.5mM, 48hrs) (A) significantly attenuated proliferation of both bovine and human PH-Fibs (n=3–6. SCR=scrambled. *, $P<0.05$; **, $P<0.01$; ***, $P<0.001$, compared to scrambled siRNA treated PH-Fibs-repeated measures ANOVA), (B) restored anti-proliferative gene (p21, p15) and pro-apoptosis gene (NOXA, PERP) expression. (n=3–6. *, $P<0.05$; **, $P<0.01$; ***, $P<0.001$, compared to scrambled siRNA treated or untreated PH-Fibs). MS metabolomic analysis (n=3) revealed that siCtBP1 and MTOB (C, D) altered the overall metabolic status of both bovine and human PH-Fibs and (E, F) showed the tendency to decrease the levels of metabolites involved in proliferative anabolic pathways (e.g. energy metabolism – AMP, ADP, orthophosphate and diphosphate; nucleotide biosynthesis, and antioxidant reactions – amino acids, glutamine/ glutamate, and pentose phosphate pathway intermediates), consistent with a less proliferative phenotype.

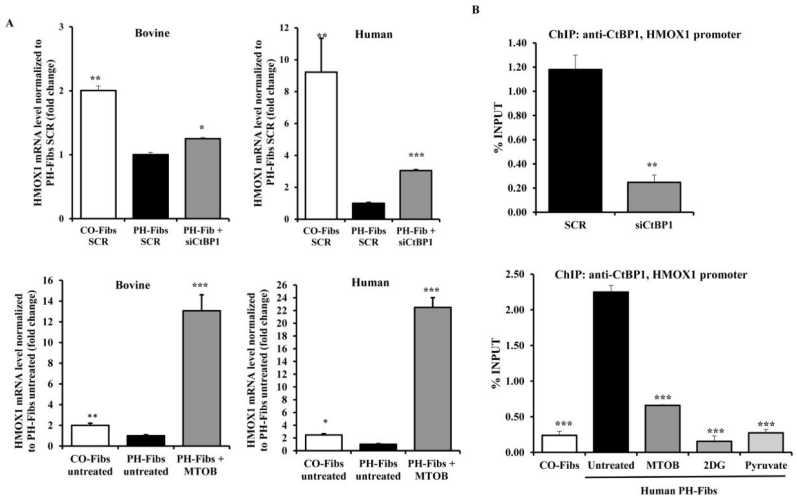

Figure 6.

CtBP1 directly regulates *HMOX1* gene expression in pulmonary artery adventitial fibroblasts. (A) Inhibition of CtBP1 by siRNA (50nM, 72hrs) or MTOB (2.5mM, 48hrs) significantly increased anti-inflammatory gene, *HMOX1*, expression in bovine and human PH-Fibs. (n=3–6. SCR=scrambled. *, $P<0.05$; **, $P<0.01$; ***, $P<0.001$, compared to scrambled siRNA treated PH-Fibs). (B) ChIP assay confirmed increased recruitment of CtBP1 to the promoter region of *HMOX1* in PH-Fibs compared to CO-Fibs. *CTBP1* siRNA attenuated precipitation of CtBP1 with *HMOX1*. 2DG, pyruvate and MTOB also suppressed binding of CtBP1 with *HMOX1*. (n=3. *, $P<0.05$; ***, $P<0.001$, compared to scrambled siRNA treated PH-Fibs or untreated PH-Fibs).

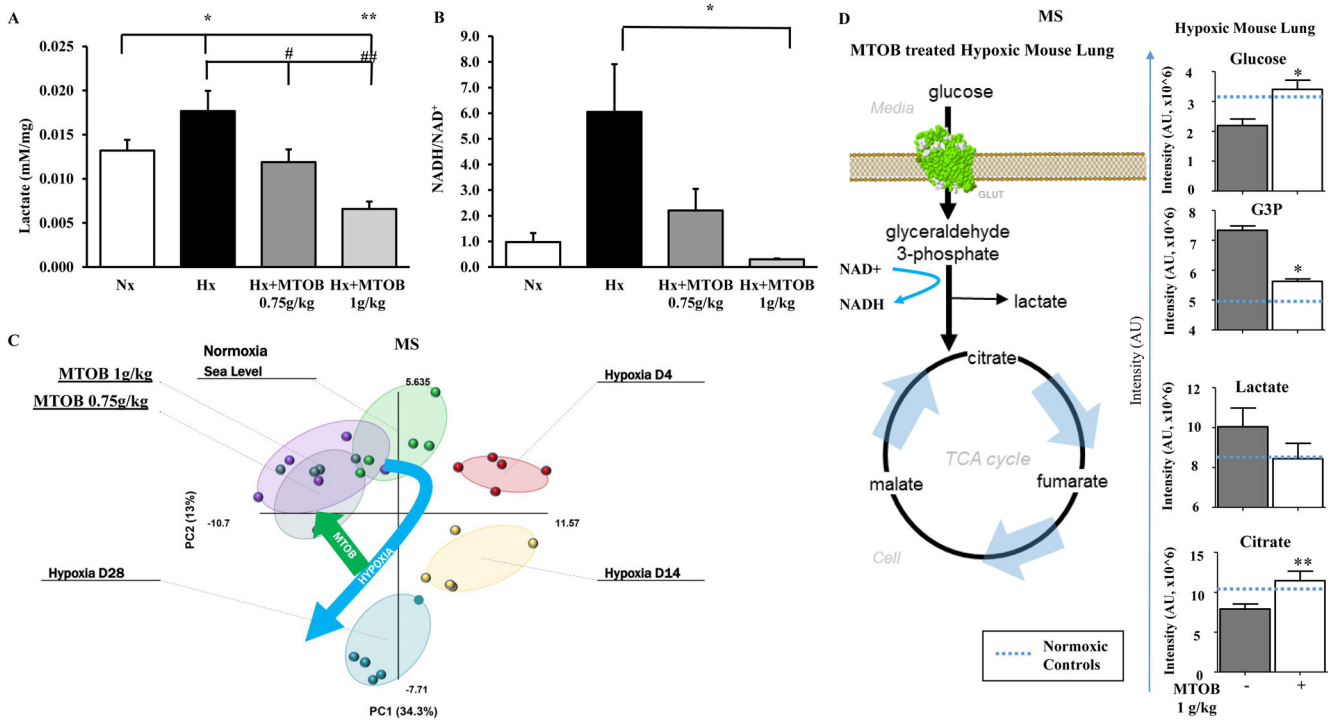

Figure 7.

Hypoxia induced glycolysis reprograming and increased NADH level in mouse lung tissue, MTOB rescued the metabolic phenotype back to normoxic controls. (A, B) Hypoxic (Hx) exposure of mice (4 days) increased lactate production and the NADH/NAD^+ ratio in whole lung tissues compared to their normoxic controls (Nx). Animals were pre-treated with MTOB for a week (3 times/week, I.P. injection with two different doses: 0.75g/kg or 1g/kg) and were received two more injections after putting into hypoxia chamber. MTOB decreased lactate level and the NADH/NAD^+ ratio in hypoxia exposed lungs (determined by enzymatic cycling reaction. n=3–5, *, $P<0.05$; **, $P<0.01$, compared to normoxic lungs; #, $P<0.05$; ##, $P<0.01$, compared to hypoxic lungs). MS metabolomic analysis discovered that (C) the overall metabolic profile of mouse lung tissue becomes increasingly altered from their normoxic state as hypoxia exposure continues and yet MTOB was able to recover the metabolic state of lung tissue back to normoxic control levels (n=5 in each group), and (D) MTOB decreased glucose consumption, glyceraldehyde-3-phosphate production, a substrate for GAPDH to generate NADH, and lactate production. (n=5, *, $P<0.05$; **, $P<0.01$, compared to MTOB untreated mouse whole lung tissue).

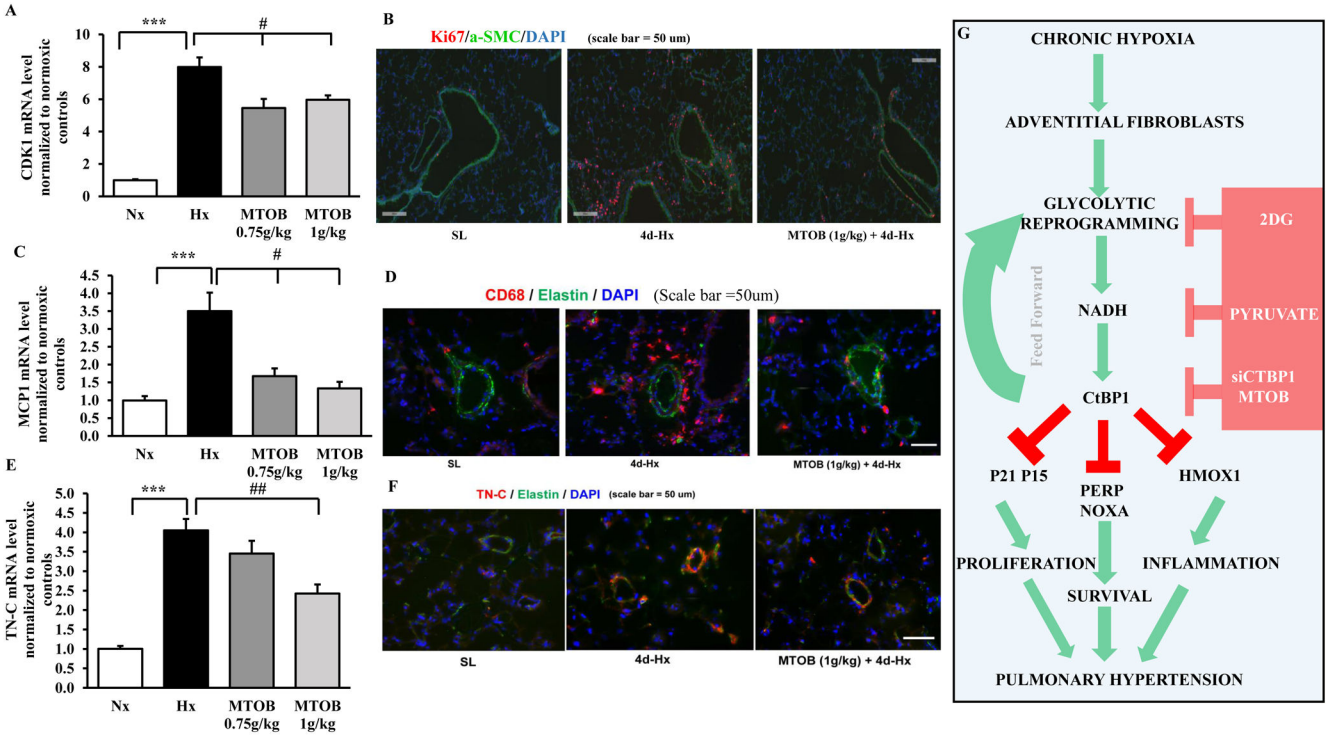

Figure 8.

Hypoxia exposure induced and MTOB treatment inhibited proliferation, inflammation and vascular remodeling in mouse lung. (A) Four day hypoxia exposure significantly increased cyclin-dependet kinase 1 (CDK1) mRNA expression in mouse whole lung tissues compared to their normoxic contols; MTOB treatment significantly decreased CDK1 levels. (B) Ki67 immunoflurescent staning (red=ki67, green=α-SMC, blue=DAPI, scale bar=50um) demonstrated that hypoxia increased and MTOB decreased cell proliferation in mouse lung tissue. (C) Four day hypoxia exposure significantly increased MCP1 mRNA expression in mouse whole lung tissues compared to their normoxic contols, and MTOB treatment significantly decreased the MCP1 level. (D) Consistent with qPCR data for MCP1, staining of the monocyte/ macrophage marker, CD68, showed hypoxia increased, and MTOB decreased, recruitment of monocytes/macrophage (red=CD68, green=elastin, blue=DAPI, scale bar=50um). (E) Four day hypoxia exposure significantly increased tenascin C (TN-C), an extra-cellular matrix marker, mRNA expression in mouse whole lung tissues compared to their normoxic contols, and MTOB treatment significantly decreased the TN-C level. (F) Accordingly, TN-C staining demonstrated MTOB attenuated vascular remodeling induced by hypoxia exposure (red=TN-C, green=elastin, blue=DAPI, scale bar=50um) (n=5, ***, P<0.001, compared to normoxic controls. #, P<0.05; ##, P < 0.01 compared to hypoxic mouse lungs). (G) CtBP1 links metabolic changes to gene expression and contributes to the development of pulmonary hypertension: pulmonary artery adventitial fibroblast cells isolated from chronic hypoxia induced pulmonary hypertensive cow model and patients with pulmonary hypertension (PH-Fibs) and maintained under normoxic conditions demonstrated a perpetuated pro-inflammatory and hyper-proliferative phenotype, as well as a metabolic reprograming towards aerobic glycolysis and subsequently increased NADH levels. The

transcriptional co-repressor activity of CtBP1 is stimulated as a result of elevated NADH level. CtBP1 then enhances cell proliferation via transcriptional repression of cell cycle inhibitors *P21, P15*, and promotes cell survival through repression of pro-apoptotic genes (*NOXA* and *PERP*). CtBP1 also induces inflammation through the repression of anti-inflammatory gene *HMOX1*. Reducing NADHs level by 2DG or pyruvate can inhibit proliferation in PH-Fibs and augment the anti-inflammatory phenotype of PH-Fibs. Targeting CtBP1 at the RNA level via siRNA or at the protein level by MTOB can not only inhibit proliferation and augment anti-inflammatory phenotype of PH-Fibs, but can also rescue cell metabolic state.

Table 1

gnificant pathways identified in the list of 1,012 differential expressed genes (p<0.01 and fold change >2) between Control and Hypertensive
by Blast2GO

Pathway	Sequences (n)	Enzymes (n)	*P*-value (Fisher's exact)	*P*-value Bonferroni	Pathway	Sequences (n)	Enzymes (n)	*P*-value (Fisher's exact)	*P*-value Bonferroni
Purine metabolism	27	17	3.06E-07	5.84E-05	Phenylalanine metabolism	4	3	0.002	0.251
tidylinositol signaling system	11	5	5.33E-07	1.02E-04	Tyrosine metabolism	4	3	0.002	0.270
colysis / Gluconeogenesis	9	10	2.10E-06	4.02E-04	Propanoate metabolism	4	3	0.002	0.310
itol phosphate metabolism	9	4	1.02E-05	0.002	Glycosaminoglycan biosynthesis – chondroitin sulfate / dermatan sulfate	4	5	0.002	0.328
lycerolipid metabolism	7	6	1.04E-05	0.002	Glycosaminoglycan degradation	4	2	0.002	0.367
Pyrimidine metabolism	7	6	2.68E-05	0.005	Pentose and glucuronate interconversions	4	4	0.003	0.384
eta-Alanine metabolism	6	5	2.76E-05	0.005	Biosynthesis of unsaturated fatty acids	3	2	0.003	0.393
Galactose metabolism	6	5	3.46E-05	0.007	Metabolism of xenobiotics by cytochrome P450	3	3	0.004	0.521
Nitrogen metabolism	5	3	6.44E-05	0.012	Chloroalkane and chloroalkene degradation	3	2	0.005	0.579
erophospholipid metabolism	5	4	1.33E-04	0.020	Streptomycin biosynthesis	3	2	0.005	0.582
se and mannose metabolism	5	5	2.12E-04	0.040	Valine, leucine and isoleucine degradation	3	2	0.005	0.625
oid hormone biosynthesis	5	4	2.42E-04	0.045	Lysine degradation	3	2	0.005	0.630
chidonic acid metabolism	4	5	3.81E-04	0.070	Starch and sucrose metabolism	3	2	0.005	0.540
Sulfur metabolism	4	4	4.46E-04	0.082	Fatty acid metabolism	3	2	0.005	0.640
metabolism - other enzymes	4	3	4.53E-04	0.065	Glycine, serine and threonine metabolism	3	2	0.005	0.554
Pyruvate metabolism	4	3	6.05E-04	0.109	Ascorbate and aldarate metabolism	3	2	0.006	0.506
Methane metabolism	4	4	0.001	0.206	Histidine metabolism	3	3	0.008	0.691
o sugar and nucleotide sugar metabolism	4	3	0.001	0.195	mTOR signaling pathway	3	2	0.009	0.666

Table 2

Genes from RNA-Seq data showing significant changes in bovine PH-Fibs compared to CO-Fibs

Gene Name	Ensembl ID	Gene Description	Fold Change	*p*-Value*
PFKFB 3	ENSBTAG00000008401	6-phosphofructo-2-kinase/fructose-2,6-biphosphatase 3	6	1.25E-05
PGM5	ENSBTAG00000033190	phosphoglucomutase-like protein 5	3.9	2.16E-06
GLUT1 /SLC2A1	ENSBTAG00000009617	Solute carrier family 2, facilitated glucose transporter member 1	2.4	7.03E-03
HK1	ENSBTAG00000012380	Hexokinase 1	2.6	4.21E-03
PFKM	ENSBTAG00000000286	6-phosphofructokinase, muscle type	2.1	2.30E-05
GPI	ENSBTAG00000006396	Glucose-6-phosphate isomerase	1.6#	2.10E-03
PFKFB 4	ENSBTAG00000006752	6-phosphofructo-2- kinase/fructose-2,6- biphosphatase 4	1.5#	1.32E-03
PGM1	ENSBTAG00000019011	Phosphoglycerate mutase 1	1.4#	6.40E-03
PGM2	ENSBTAG00000005773	Phosphoglycerate mutase 2	1.3#	8.04E-03
ID1	ENSBTAG00000016169	DNA-binding protein inhibitor ID-1	−5.78	9.35E-04
ID2	ENSBTAG00000021187	DNA-binding protein inhibitor ID-2	−4.25	4.92E-04
SIRT4	ENSBTAG00000021168	NAD-dependent protein deacetylase sirtuin-4	−1.3#	4.80E-03
RGS5	ENSBTAG00000016341	Regulator of G-protein signaling 5	551.37	1.56E-04

*The presented p-values have q-value <0.1 (false discovery rate, FDR)

#These genes are related to the function of CtBP1, the phenotype of fibroblast cells, or are also important genes involved in glycolysis, even with a fold change of less than 2.